Nature Letter, 20 January 2011, 000, 000–000

Supermassive black holes do not correlate with dark matter halos of galaxies

John Kormendy[1,2,3] & Ralf Bender[2,3]

Supermassive black holes have been detected in all galaxies that contain bulge components when the galaxies observed were close enough so that the searches were feasible. Together with the observation that bigger black holes live in bigger bulges[1–4], this has led to the belief that black hole growth and bulge formation regulate each other[5]. That is, black holes and bulges "coevolve". Therefore, reports[6,7] of a similar correlation between black holes and the dark matter halos in which visible galaxies are embedded have profound implications. Dark matter is likely to be nonbaryonic, so these reports suggest that unknown, exotic physics controls black hole growth. Here we show – based in part on recent measurements[8] of bulgeless galaxies – that there is almost no correlation between dark matter and parameters that measure black holes unless the galaxy also contains a bulge. We conclude that black holes do not correlate directly with dark matter. They do not correlate with galaxy disks, either[9,10]. Therefore black holes coevolve only with bulges. This simplifies the puzzle of their coevolution by focusing attention on purely baryonic processes in the galaxy mergers that make bulges[11].

The idea of coevolution was motivated by the observation that bigger black holes (BHs) live in bulges and elliptical galaxies that have bigger velocity dispersions σ at large radii where stars feel mainly each others' gravity and not that of the BH[3,4]. This correlation was compelling, because its scatter was small, consistent with measurement errors. The reduced χ^2 was 0.79 for the highest-accuracy sample[3], and "the intrinsic scatter [in BH mass $M_\bullet$ at fixed σ] is probably less than 0.15 dex."[4] The scatter was so small that σ could be used as a surrogate for $M_\bullet$ for many arguments. More important was the implication that a fundamental physical connection between BH and bulge growth awaits discovery, given the realization[12] that even a tiny fraction of the energy produced in BH growth could, if absorbed by protogalactic gas, regulate bulge formation. Small scatter will be important here, too. Tight correlations motivate a search for underlying physics. Loose correlations are less compelling: bigger galaxies just tend to be made of bigger galaxy parts.

The discovery[6,7] of a similarly tight correlation between σ and the circular rotation velocities V_{circ} of gas in the outer parts of galaxies, where gravity is controlled by dark matter (DM), therefore was taken to imply that DM also regulates BH growth. In fact, it was suggested[6] that the more fundamental correlation is the one with DM; i. e., that dark matter engineers coevolution.

The proposed BH–DM correlation raised two concerns. First, it was known that BHs do not correlate with galaxy disks[9], whereas galaxy disks correlate closely with DM[13,14]. It was not clear how BHs and disks could separately correlate with DM without also correlating with each other. Second, the velocity resolution of some σ measurements was too low to resolve narrow spectral lines; this problem is discussed in the caption to Figure 1.

If dark matter controls BH growth and bulges are essentially irrelevant, then V_{circ} should correlate tightly with σ even in galaxies that do not have bulges. Figure 1 performs this test.

Figure 1 updates the plot that was used to claim[6] a BH – DM correlation. The reliable original data are shown in black; points measured with low velocity resolution were omitted as documented in Supplementary Table 1. Motivated by the above discussion, we measured[8] velocity dispersions in six Sc – Scd galaxies that have nuclear star clusters ("nuclei") but essentially no bulges. They are shown by red points. Other color points show additional published data on bulgeless galaxies that were measured with enough spectral dispersion to resolve nuclear σ.

Figure 1 shows that bulgeless galaxies (color points, NGC 3198) show only a weak correlation between V_{circ} and σ. This is expected, because bigger galaxies tend to have bigger nuclei[20]. But no tight correlation suggests any more compelling formation physics than the expectation that bigger nuclei can be manufactured in bigger galaxies that contain more fuel. The

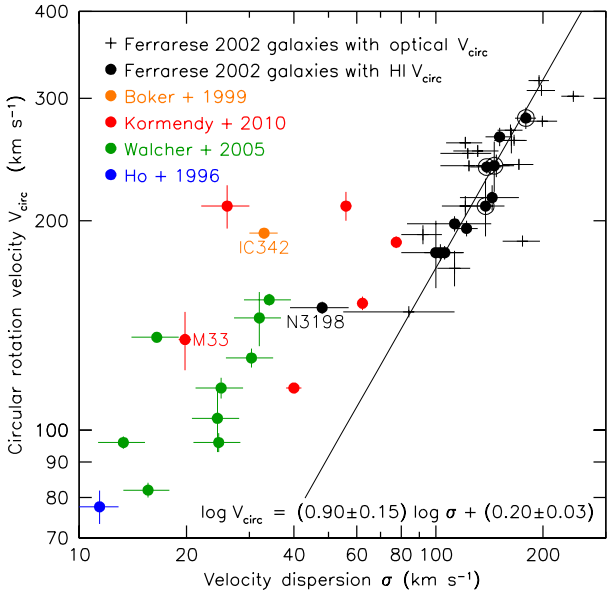

Figure 1 | Outer rotation velocity V_{circ} vs. near-central velocity dispersion σ. The data are listed in the Supplementary Information. Error bars are 1 sigma. The original BH–DM correlation[6] is shown in black symbols (circled if the galaxy has a classical bulge) except that points have been omitted if the σ measurement had insufficient velocity resolution. For example, the bulgeless Scd galaxy IC 342 (now the orange point, after correction) was shown[6] at σ = 77 ± 12 km s^{-1}, consistent with the black points. But the measurement[15] had low resolution: the instrumental velocity dispersion σ_{instr} = (resolution FWHM)/2.35 was 61 km s^{-1}, similar to σ found in IC 342. Low resolution often results in overestimated σ. The same source lists σ = 77 km s^{-1} for the nucleus of M 33, which has σ = 21 ± 2 km s^{-1} as measured at high resolution[16,17]. In fact, a high resolution measurement of IC 342 was available[18]: at σ_{instr} = 5.5 km s^{-1}, σ is observed to be 33 ± 3 km s^{-1} (orange point). We correct or omit black points if $\sigma \lesssim \sigma_{instr}$. We add points (color) for galaxies measured with $\sigma_{instr} < 10$ km s^{-1}, i. e., high enough resolution to allow measurement of the smallest dispersions seen in galactic nuclei. The line (equation at bottom; velocities are in units of 200 km s^{-1}) is a symmetric least-squares fit[19] to the black filled circles minus NGC 3198. It has χ^2 = 0.25. The correlation coefficient is r = 0.95. This correlation is at least as good as $M_\bullet - \sigma$. The correlation for the + points has χ^2 = 2.6 and r = 0.77. In contrast, the correlation for the color points plus NGC 3198 has χ^2 = 15.7 and r = 0.70.

[1]Department of Astronomy, University of Texas at Austin, 1 University Station, Austin, TX 78712-0259, USA

[2]Max-Planck-Institut für Extraterrestrische Physik, Giessenbachstrasse, D-85748 Garching-bei-München, Germany

[3]Universitäts-Sternwarte, Scheinerstrasse 1, D-81679 München , Germany

scatter is much larger than the measurement errors, $\chi^2 = 15.7$. Note in particular that galaxies with $\sigma \simeq 25$ km s^{-1} span almost the complete V_{circ} range for the color points, 96 – 210 km s^{-1}.

Our measurements[8] were made with the 9.2 m Hobby-Eberly Telescope and High Resolution Spectrograph; $\sigma_{instr} = 8$ km s^{-1} reliably resolves the smallest velocity dispersions seen in galactic nuclei. We easily confirm that $\sigma = 19.8 \pm 0.7$ km s^{-1} in M 33 and include this value in Figure 1.

Two properties of our sample deserve emphasis. First, we observed NGC 5457 = M 101 and NGC 6946, because these are among the biggest bulgeless galaxies ($V_{circ} \simeq 210$ km s^{-1}). This is important because Ferrarese concluded[6] that "the V_{circ}–σ relation ... seems to break down below $V_{circ} \sim 150$ km s^{-1} [in our notation, so] halos of mass smaller than $\sim 5 \times 10^{11}\, M_\odot$ are increasingly less efficient at forming BHs." Our galaxies show that $V_{circ} - \sigma$ breaks down already at $V_{circ} = 210$ km s^{-1} if the galaxy contains no bulge.

Second, our sample is intentionally biased against galaxies that contain bulges. We even avoided substantial "pseudobulges"; i. e., "fake bulges" that were made by the internal evolution of galaxy disks[21] rather than by the galaxy mergers that make "classical bulges". The pseudobulge-to-total mass ratios of our galaxies are $\lesssim$ a few percent; the bulge-to-total ratios are zero. The relevance of pseudobulges is discussed below. We chose these galaxies because, as noted earlier, *we want to know whether DM correlates with BHs in the absence of the component that we know correlates with BHs.* A study[22] of a large galaxy sample that is not biased against bulges results in similar conclusions: V_{circ} correlates weakly with σ, especially at Hubble types where galaxies contain classical bulges, but the scatter is large and "these results render questionable any attempt to supplant the bulge with the halo as the fundamental determinant of the central black hole mass in galaxies.[22]" Results from this study are included in Figure S3 in the Supplementary Information.

Figure 1 shows substantial overlap in V_{circ} between the color points that show little correlation and the black filled circles that show a good correlation with σ. (The black points shown as error bars are for galaxies with only optical rotation curves; they measure V_{circ} less accurately, because they reach less far out into the DM halo[6]. They show a weak correlation that is not a compelling argument for coevolution.) In the overlap range, 180 km s^{-1} $\lesssim V_{circ} \lesssim$ 220 km s^{-1}, galaxies participate in the tight $V_{circ} - \sigma$ shown by the black filled circles only if they contain bulges. Clearly baryons matter to BH growth. But baryons in a disk are not enough. DM by itself is not enough. M 101 (top-left red point) has a halo that is similar to those of half of the galaxies in the tight correlation, but that halo did not manufacture a canonical BH in the absence of a bulge. This suggests that bulges, not halos, coevolve with BHs.

Nevertheless, most black circles in Figure 1 show a correlation whose scatter is consistent with the error bars. We need to understand this.

We suggest that the tight correlation of black points in Figure 1 is a result of the well known conspiracy[13,14] between baryons and DM to make featureless rotation curves with no distinction between the parts that are dominated by baryonic and nonbaryonic matter. This possibility was considered and dismissed in reference (6). However, it is a natural consequence of the observation that baryons make up 17 % of the matter in galaxies[23] and that, to make stars, they need to dissipate inside their halos until they are self-gravitating. This is enough to engineer that V_{circ} is approximately the same for DM halos and for disks embedded in them[24,25]. That part of the conspiracy is not shown by Figure 1 because, absent a bulge, disks reach V_{circ} at large radii that are not sampled by σ measurements of nuclei.

Bulges dissipate more than disks. The consequences are shown in Figures S1 and S2 in the Supplementary Information. Figure S1 shows that V_{circ} for the bulge $\approx V_{circ}$ for the halo for the two highest-V_{circ} galaxies whose points are circled in Figure 1. Figure S2 shows that the same equality holds reasonably well, given the uncertainties in rotation curve decomposition, for all decompositions that we could find that included a bulge. It holds in just the V_{circ} range, 180 – 260 km s^{-1}, where the black circles in Figure 1 show a tight correlation. Because a bulge has $V_{circ} \sim \sqrt{2}\sigma$, a correlation like that in Figure 1 is expected from Figure S2. *All galaxies that participate in the tight correlation in Figure 1 are included in Figure S2. And all of them have bulges or pseudobulges. We conclude that the correlation is nothing more nor less than a restatement of the rotation curve conspiracy for bulges and DM.* It is a consequence of DM-mediated galaxy formation. The conceptual leap to a direct causal correlation between DM and BHs is not required by the data.

So far, we have discussed BH correlations indirectly using the assumption that σ is a surrogate for BH mass. We now check this assumption and show that it is not valid for most of the black points that define the tight correlation in Figure 1. If σ is not a measure of $M_\bullet$, then this further shows that the correlation is not a consequence of a BH – DM coevolution.

In Figure 2, we examine directly the correlations between $M_\bullet$ and host galaxy properties for galaxies in which BHs have been detected dynamically. All plotted parameters are published elsewhere. The galaxy sample and plotted data are listed in the Supplementary Information of the accompanying Letter[10]. The same galaxies are shown in all panels except: ellipticals do not appear in panel (c) because they have no disk; bulgeless galaxies do not appear in panel (a) because they have no bulge; some bulgeless galaxies and pseudobulge galaxies with $M_\bullet$ limits do not appear in panel (b) because σ is outside the plot range.

The top panels correlate $M_\bullet$ with the (a) luminosity and (b) velocity dispersion of the host-galaxy bulge. Ellipticals (black) and classical bulges (red) show the (a) good and (b) better correlations that we have come to expect.

Figure 2(c) shows[10] that galaxy disks do not correlate with $M_\bullet$. Disks participate in the rotation curve conspiracy: they and their DM halos have similar V_{circ}. But their masses – represented here by their K-band luminosities – cannot be used to predict $M_\bullet$.

Figure 2 also distinguishes "classical bulges" (red points) and "pseudobulges" (blue points). Classical bulges are essentially indistinguishable in structure and parameter correlations from elliptical galaxies (black points). We believe that both formed by galaxy mergers (see below). Pseudobulges are high-density, central components in galaxies that superficially resemble – and often are mistaken for – classical bulges but that can be recognized because their properties are more disk-like than those of classical bulges. We now know that this results from fundamentally different formation histories. Complementary to hierarchical clustering[26], a new aspect of our understanding of galaxy formation[21] is that isolated galaxy disks evolve slowly as nonaxisymmetries such as bars redistribute angular momentum. During this process, pseudobulges are grown out of disk material. Bulge-pseudobulge classifications are listed for all objects in the sample in the Supplemental Information of reference (10). Panels (a) and (b) of Figure 2 illustrate a conclusion from that Letter which has consequences here: Pseudobulges show essentially no correlation between $M_\bullet$ and σ. Baryons do not predict $M_\bullet$ if they are in a pseudobulge.

If $M_\bullet$ and σ do not correlate for pseudobulges, then σ is not a surrogate for $M_\bullet$ in Figure 1, either. Bulge classifications for the Figure 1 galaxies are given in the Supplementary Information of this paper, and two galaxies with no published data are classified.

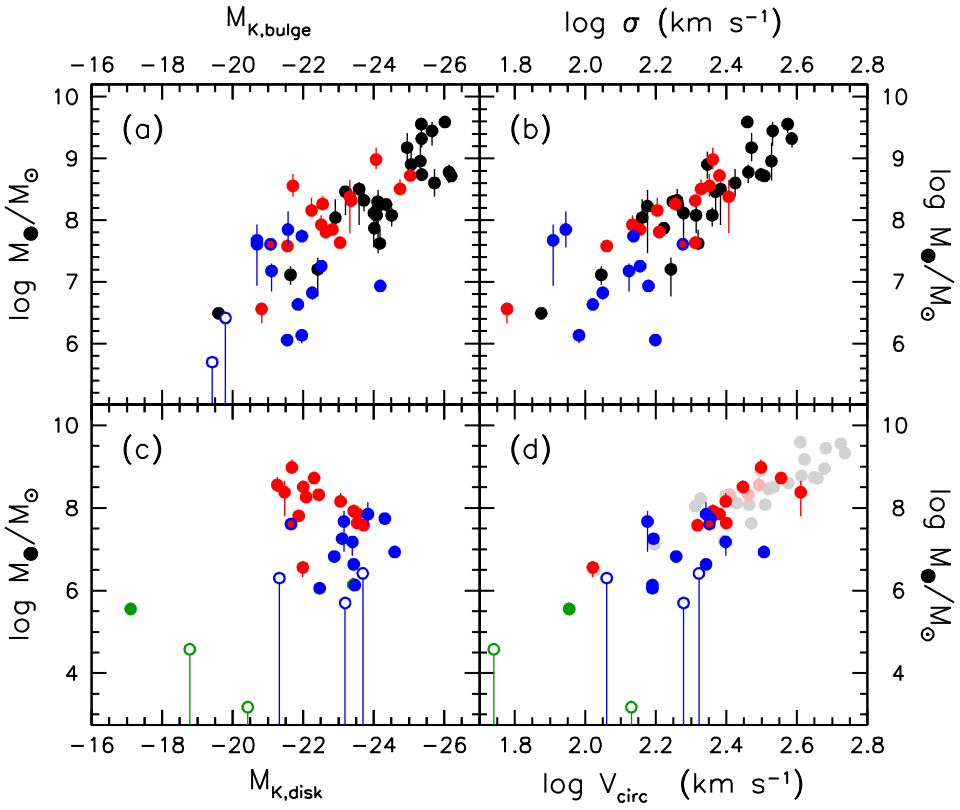

Figure 2 | Correlations of dynamically measured black hole masses with structural parameters of host galaxies. Panel (a) shows BH mass $M_\bullet$ versus the K-band absolute magnitude of the host galaxy bulge with disk light removed. Panel (b) shows $M_\bullet$ versus the velocity dispersion of the host bulge averaged inside the radius that contains one-half of the bulge light. Elliptical galaxies are plotted in black; classical bulges are plotted in red, and pseudobulges are plotted in blue. Green points are for galaxies that contain neither a classical nor a large pseudo bulge but only a nuclear star cluster. The lower panels show the analogous correlations for the disks of host galaxies. Panel (c) shows $M_\bullet$ versus the absolute magnitude of the disk with bulge light removed, and panel (d) shows $M_\bullet$ versus outer rotation velocity V_{circ}. Panels (a) – (c) are from a parallel paper[10]; all data plotted here are tabulated there in the Supplementary Information. Errors bars are 1 sigma. Based on these, in panel (a), classical bulges and ellipticals together have χ^2 = 12.1 and r = -0.82; this is the well known good correlation and is consistent with previous derivations[27]. We assume 1-sigma errors in M_K of $\pm$ 0.05 mag. Similarly, in (b), the red and black points have χ^2 = 5.0 and r = 0.89 implying an intrinsic scatter in log $M_\bullet$ of 0.26 at fixed σ to reduce χ^2 to 1.0. This also is consistent with previous derivations[19,27]. It is the good correlation that motivates our ideas about BH – bulge coevolution. In contrast, pseudobulges do not correlate with $M_\bullet$; in panel (a), the blue points have χ^2 = 63 and r = 0.27, and in panel (b), they have χ^2 = 10.4 and r = -0.08. Similarly[10], disks do not correlate with $M_\bullet$: in panel (c), the red and blue points together have χ^2 = 81 and r = 0.41. Formally, $M_\bullet$ and disk luminosity anticorrelate, but this is not significant. Finally, in panel (d), the blue points have χ^2 = 11 and r = 0.29: they show no correlation. In contrast, the red points for classical bulges show a correlation that, we argue, is a restatement of the rotation curve conspiracy. Here, elliptical galaxies and some S0s are plotted in light gray and pink, respectively, because V_{circ} is not known. We therefore plot the surrogate quantity $\sqrt{2}\sigma$, and it agrees with the correlation seen for bulges that have V_{circ} measurements. Panel (d) is a direct demonstration that, absent bulges, BHs do not correlate with DM.

We find that only four black circles in Figure 1 correspond to classical bulges, M 31, NGC 2841, NGC 4258, and NGC 7331. Their points are circled. The others are for pseudobulges. For these, the demonstration of a tight $V_{circ} - \sigma$ correlation is not a demonstration that DM and BHs correlate.

Instead, if V_{circ} correlates with σ but σ does not measure $M_\bullet$, then this supports our conclusion that the correlation results from the rotation curve conspiracy. Also, the circled points for classical bulges agree with the correlation for pseudobulges. It is implausible to suggest that the correlation for circled points is caused by BH – DM coevolution whereas the identical correlation for the other points has nothing to do with BHs.

Finally, Figure 2(d) shows directly that $M_\bullet$ does not correlate with V_{circ} and therefore with dark matter for pseudobulges.

An additional argument is given in § 3 of the Supplementary Information. If DM V_{circ} predicts $M_\bullet$ independent of baryon content, then the $V_{circ} \sim 1400$ km s^{-1} DM in clusters of galaxies predicts BHs of mass $M_\bullet \sim 7 \times 10^{11}$ $M_\odot$ that are impossible to hide in well studied clusters such as Coma.

Therefore, over the whole range of V_{circ} values associated with dark matter, i. e., at least 50 – 2000 km s^{-1}, Figure 2(d) shows a correlation with $M_\bullet$ only from 200 – 400 km s^{-1} plus NGC 7457 at 105 km s^{-1}, but only if the galaxy contains a classical bulge. The bulge correlation can be understood as an indirect result of the rotation curve conspiracy. Even in the above V_{circ} range, there is no correlation if the galaxy has only a pseudobulge or disk. Baryons are not irrelevant. They are not even sufficient. To correlate with $M_\bullet$, they must be in a classical bulge or elliptical.

We conclude that BHs do not correlate causally with DM halos. There is no reason to expect that the unknown, exotic physics of non-baryonic dark matter directly affects BH growth. Even DM gravity is not directly responsible for BH – galaxy coevolution. Rather, that coevolution appears to be as simple as it could be:

BHs coevolve only with classical bulges and ellipticals. We have a well developed picture of the their formation. Hierarchical clustering of density fluctuations in cold dark matter results in frequent galaxy mergers[11,26,28]. The products of roughly equal-mass mergers are classical bulges and ellipticals, because

progenitor disks get scrambled away by dynamical violence[11]. During this process, gas falls to the center, triggers a burst of star formation[29,30], and builds the high stellar densities that we see in bulges. This gas may also feed black holes. In fact, we see a correspondence[29] between mergers-in-progress and quasar-like nuclear activity that builds $M_\bullet$. Our increasingly persuasive picture is that the growth of black holes and the assembly of ellipticals happen together and regulate each other[12,30]. The present results support this picture.

Received 15 July; accepted 15 November 2010.

1. Kormendy, J. A critical review of stellar-dynamical evidence for black holes in galaxy nuclei. in *The Nearest Active Galaxies*. (eds Beckman, J., Colina, L., & Netzer, H.) 197–218 (Madrid: Consejo Superior de Investigaciones Científicas, 1993).
2. Kormendy, J. & Richstone, D. Inward bound – The search for supermassive black holes in galactic nuclei. *Annu. Rev. Astron. Astrophys.* **33**, 581–624 (1995).
3. Ferrarese, L. & Merritt, D. A fundamental relation between supermassive black holes and their host balaxies. *Astrophys. J.* **539**, L9–L12 (2000).
4. Gebhardt, K., *et al.* A relationship between nuclear black hole mass and galaxy velocity dispersion. *Astrophys. J.* **539**, L13–L16 (2000).
5. Ho, L. C., Ed. *Carnegie Observatories Astrophysics Series, Volume 1: Coevolution of Black Holes and Galaxies* (Cambridge Univ. Press, 2004).
6. Ferrarese, L. Beyond the bulge: A fundamental relation between supermassive black holes and dark matter halos. *Astrophys. J.* **578**, 90–97 (2002).
7. Baes, M., Buyle, P., Hau, G. K. T. & Dejonghe, H. Observational evidence for a connection between supermassive black holes and dark matter haloes. *Mon. Not. R. Astron. Soc.* **341**, L44-L48 (2003).
8. Kormendy, J., Drory, N., Bender, R. & Cornell, M. E. Bulgeless giant galaxies challenge our picture of galaxy formation by hierarchical clustering. *Astrophys. J.* **723**, 54–80 (2010).
9. Kormendy, J. & Gebhardt, K. Supermassive black holes in galactic nuclei. in *20*$^{\rm th}$ *Texas Symposium on Relativistic Astrophysics*. (eds Wheeler, J. C. & Martel, H.) 363–381 (AIP, 2001).
10. Kormendy, J., Bender, R. & Cornell, M. E. Supermassive black holes do not correlate with galaxy disks or pseudobulges. *Nature* **000**, 000–000 (2011).
11. Toomre, A. Mergers and some consequences. in *Evolution of Galaxies and Stellar Populations* (eds Tinsley, B. M. & Larson, R. B.) 401–426 (Yale University Observatory, 1977).
12. Silk, J. & Rees, M. J. Quasars and galaxy formation. *Astron. Astrophys.* **331**, L1–L4 (1998).
13. van Albada, T. S. & Sancisi, R. Dark matter in spiral galaxies. *Phil. Trans. R. Soc. London A* **320**, 447–464 (1986).
14. Sancisi, R. & van Albada, T. S. H I rotation curves of galaxies. in *IAU Symposium 117, Dark Matter in the Universe* (eds Kormendy, J. & Knapp, G. R.) 67–81 (Reidel, 1987).
15. Terlevich, E., Díaz, A. I. & Terlevich, R. On the behaviour of the IR Ca II triplet in normal and active galaxies. *Mon. Not. R. Astron. Soc.* **242**, 271–284 (1990).
16. Kormendy, J. & McClure, R. D. The nucleus of M 33. *Astron. J.* **105**, 1793–1812 (1993).
17. Gebhardt, K., *et al.* M 33: A galaxy with no supermassive black hole. *Astron. J.* **122**, 2469–2476 (2001).
18. Böker, T., van der Marel, R. P. & Vacca, W. D. CO band head spectroscopy of IC 342: Mass and age of the nuclear star cluster. *Astron. J.* **118**, 831–842 (1999).
19. Tremaine, S., *et al.* The slope of the black hole mass versus velocity dispersion correlation. *Astrophys. J.* **574**, 740–753 (2002).
20. Böker, T., *et al.* A Hubble Space Telescope census of nuclear star clusters in late-type spiral galaxies. II. Cluster sizes and structural parameter correlations. *Astron. J.* **127**, 105–118 (2004).
21. Kormendy, J. & Kennicutt, R. C. Secular evolution and the formation of pseudobulges in disk galaxies. *Annu. Rev. Astron. Astrophys.* **42**, 603–683 (2004).
22. Ho, L. C. Bulge and halo kinematics across the Hubble sequence. *Astrophys. J.* **668**, 94–109 (2007).
23. Komatsu, E., *et al.* Five-year Wilkinson Microwave Anisotropy Probe observations: Cosmological interpretation. *Astrophys. J. Suppl. Ser.* **180**, 330–376 (2009).
24. Gunn, J. E. Conference summary. in *IAU Symposium 117, Dark Matter in the Universe* (eds Kormendy, J. & Knapp, G. R.) 537–546 (Reidel, 1987).
25. Ryden, B. S. & Gunn, J. E. Galaxy formation by gravitational collapse. *Astrophys. J.* **318**, 15–31 (1987).
26. White, S. D. M. & Rees, M. J. Core condensation in heavy halos: A two-stage theory for galaxy formation and clustering. *Mon. Not. R. Astron. Soc.* **183**, 341–358 (1978).
27. Gültekin, K., *et al.* The M–σ and M–L relations in galactic bulges, and determinations of their intrinsic scatter. *Astrophys. J.* **698**, 198–221 (2009).
28. Springel, V. Simulations of the formation, evolution and clustering of galaxies and quasars. *Nature* **435**, 629–636 (2005).
29. Sanders, D. B., Soifer, B. T., Elias, J. H., Madore, B. F., Matthews, K., Neugebauer, G. & Scoville, N. Z. Ultraluminous infrared galaxies and the origin of quasars. *Astrophys. J.* **325**, 74–91 (1988).
30. Hopkins, P. F., Hernquist, L., Cox, T. J., di Matteo, T., Robertson, B. & Springel, V. A unified, merger-driven model of the origin of starbursts, quasars, the cosmic X-ray background, supermassive black holes, and galaxy spheroids. *Astrophys. J. Suppl. Ser.* **163**, 1–49 (2006).

Supplementary Information is linked to the online version of the paper at www.nature.com/nature.

Acknowledgments We thank Stephane Courteau for making available his surface photometry of NGC 801 (S. I.) and Jenny Greene for helpful comments on the MS. The Hobby-Eberly Telescope (HET) is a joint project of the University of Texas at Austin, Pennsylvania State University, Stanford University Ludwig-Maximilians-Universität Munich, and Georg-August-Universität Göttingen. The HET is named in honor of its principal benefactors, William P. Hobby and Robert E. Eberly. This work was supported by the National Science Foundation.

Author Contributions Both authors contributed to the analysis in this paper. J.K. wrote most of the text.

Author Information Reprints and permissions information is available at www.nature.com/reprints. The authors declare no competing financial interests. Correspondence and requests for materials should be addressed to J.K. (kormendy@astro.as.utexas.edu).

Supplementary Information

We expand on four issues: § 1 explains the consequences for this paper of the "conspiracy" *in the biggest disk galaxies* that bulges, disks, and dark matter halos are arranged in density and radius so that their combined, circular-orbit rotation curves are almost flat. Section 2 reconstructs Figure 1 for the rotation curve sample used in Section 1 and updates it with newer and more accurate measurements. The result (Fig. S3) is that the strong $V_{circ} - \sigma$ correlation at high V_{circ} in Figure 1 looks weaker. Section 3 presents an additional argument that dark matter does not predict $M_\bullet$ irrespective of the nature and amount of its baryon content. Finally, § 4 documents the data used to construct Figure 1.

1. The Conspiracy Between Visible and Dark Matter To Produce Flat, Featureless Rotation Curves

Figure S1 illustrates the rotation curve conspiracy[13,14,31] in the highest- and third-highest-V_{circ} galaxies in Figure 1. In NGC 2841, in M 31, and in high-V_{circ} galaxies in general, bulges, disks, and DM halos are arranged in radius and density so that their combined rotation curves are so flat and featureless that one cannot easily tell which component dominates at which radius. To understand rotation curves, it is necessary to decompose them into the contributions from each component[32]. Rotation curve decompositions like those illustrated in Figure S1 are available for all of the galaxies in Figure 1 that have H I measurements of V_{circ}.

A slightly oversimplified paraphrase of the conspiracy is that each component has approximately the same maximum V_{circ}. But they reach these maxima at different radii – the bulge near the center, then the disk (including gas) and then the DM at radii that are usually outside the visible part of the galaxy (Figure S1). The important conclusion is this: If $V_{circ,bulge} \simeq V_{circ,halo}$ (in obvious notation), then there is no reason to believe that any $V_{circ} - \sigma$ correlation that remains at high rotation velocities in Fig. 1 is a correlation of σ and hence $M_\bullet$ with DM. It may be no more than the correlation with bulges that we already know about.

In particular, three of the four highest-V_{circ} galaxies in Figure 1 contain classical bulges. They are, from top to bottom, NGC 2841, M 31, and NGC 7331. The fourth is NGC 4565, which has both a big boxy pseudobulge – i. e., an edge-on bar – and a smaller "disky" pseudobulge[33]. Some of the biggest pseudobulges are consistent with the BH-host galaxy correlations in the top panels of Figure 2.

To rephrase our conclusion: We suggest that any $V_{circ} - \sigma$ correlation that remains in Figure 1 is due to the rotation curve conspiracy. Ferrarese[6] considered but dismissed this possibility. However, we can test our suggestion, because bulges dominate the biggest galaxies and then disappear as galaxy luminosity decreases. If we are correct, then we expect that any correlation in Figure 1 breaks down at V_{circ} values where bulges become unimportant. We show in Figure S2 that this happens at $V_{circ} \ll 200$ km s^{-1}.

The key to our test is that the rotation curve conspiracy is not perfect[31]: it works best for intermediate-luminosity galaxies, but at large radii, "rotation curves rise for faint[er] galaxies, fall for bright[er] ones." Rephrased in the language of Figure S1, V_{circ} for the central component(s) is smaller than that of the halo in the smallest galaxies and larger than that of the halo in the biggest galaxies. We illustrate this point in Figure S2 and then show why it is relevant to our argument.

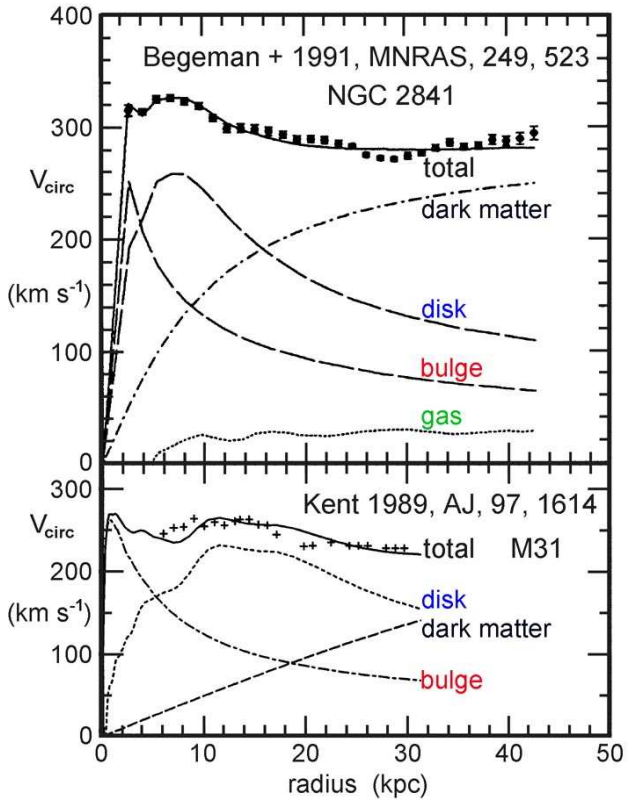

Figure S1 | Rotation curve decompositions for two galaxies in Figure 1 that have classical bulges and $V_{circ} > 200$ km s^{-1}. The standard technique[32] is to determine the bulge and disk rotation curves from their radial brightness distributions via the assumption that their mass-to-light ratios M/L are constant with radius. Generally (top) but not always (bottom), H I gas is explicitly taken into account. The total rotation curve is the sum in quadrature of its components, i. e., $V_{circ}^2(r) = V_{circ,bulge}^2 + V_{circ,disk}^2 + V_{circ,gas}^2$. This visible-matter rotation curve fits only the central part of the observed rotation curve, some of which is shown by the data points. One of the strongest pieces of evidence for dark matter[34] is that the visible matter cannot explain the flat rotation curve at large radii. Outside the visible matter – i. e., well outside the maxima in V_{circ} for visible components – the total rotation curve should become Keplerian, $V_{circ} \propto r^{-1/2}$. This is the behavior of the bulge rotation curves in Figure S1, because most radii shown are outside most bulge mass. Because the total rotation curve stays flat rather than becoming Keplerian, sufficient dark matter must live at large radii so that the new sum in quadrature of V_{circ} for all components fits the data. There are two big uncertainties in measuring this dark matter[32,35]. Most important are the unknown M/L values. A procedure with substantial[36-41] but not bomb-proof[32,42-44] justification is the "maximum disk assumption" in which bulge and disk M/L values are set to the largest values that do not over-predict the central rotation curve. Figure S1 illustrates these maximum disk = minimum halo models. The unknown values and radial dependences of M/L exacerbate the second problem, which is that the radial density distribution $\rho(r)$ of the dark matter is not known. The usual practice is to assume a functional form for $\rho(r)$ and then scale the parameters of the halo until it adds up with the visible matter to fit the observed rotation curve. In this paper, we use decompositions based on isothermal dark halos or their equivalent[41]. Consistent use of different halo models would lead to somewhat different decompositions quantitatively but the same qualitative trends with galaxy luminosity and outer V_{circ}. In the decompositions illustrated, we assume that the rotation curve of the dark matter converges to the flat outer rotation velocity observed. The conclusion from the decompositions – and our point in this section – is that, for each galaxy, the maximum V_{circ} is approximately the same for the bulge, the disk, and the dark halo.

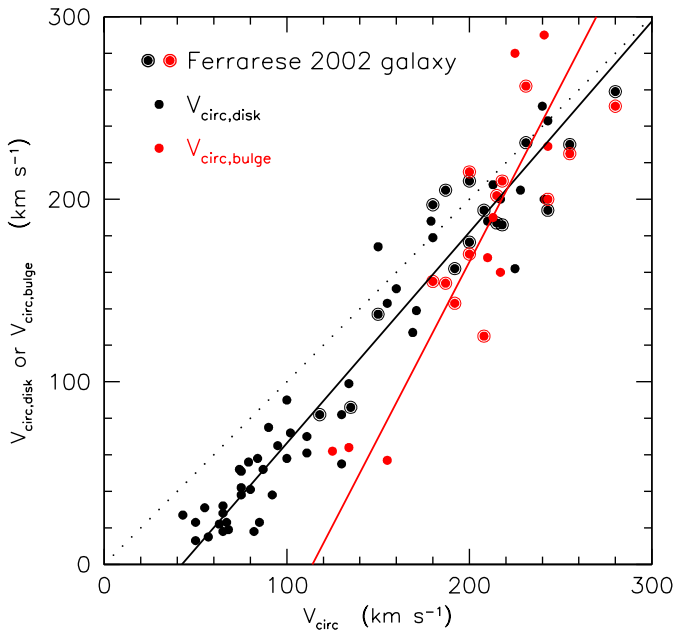

Figure S2 | Maximum rotation velocities of the bulge $V_{circ,bulge}$ (red points) and disk $V_{circ,disk}$ (black points) given in bulge-disk-halo decompositions of observed rotation curves whose outer rotation velocities are V_{circ}. Here V_{circ} is assumed to be the maximum rotation velocity of the dark matter. The sparse dotted line indicates equality of the visible matter and dark matter maximum rotation velocities. Every red point has a corresponding black point, but many galaxies are sufficiently bulgeless so that only a disk was included in the decomposition and then the plot shows only a black point. This is universally true for the smallest galaxies; they never contain bulges. The rotation curve conspiracy happens for galaxies with $V_{circ} \sim 200$ km s^{-1}: this is where $V_{circ,bulge} \simeq V_{circ,disk} \simeq V_{circ}$ for the halo. The correlation for bulges is steeper than that for disks; i. e., bulges disappear rapidly at lower rotation velocities. The lines are least-squares fits such that the adopted relation y(x) is the mean of a regression of y on x and one of x on y, where each variable has first been symmetrized approximately around its mean[19]. The sample is small, but the regressions hint that $V_{circ,bulge}$ tends to be bigger than both $V_{circ,disk}$ and V_{circ} in the biggest galaxies; this helps to explain why these galaxies have outward-falling rotation curves[31]. Similarly, $V_{circ,disk} < V_{circ}$ in the smallest galaxies; this is the other half of the conspiracy's breakdown[31]. In fact, the baryonic components disappear almost entirely at $V_{circ} \sim 45$ km s^{-1}; this is an illustration of the well known observation that the smallest galaxies are completely dominated by dark matter[41]. The important point for the present paper is that $V_{circ} \gtrsim 200$ km s^{-1} is just as much a parameter of the bulge as it is a parameter of the dark matter halo. All galaxies represented by black filled circles in Figure 1 are also included in Figure S2 (circled points). Therefore our conclusions apply to these galaxies.

To check whether the results in Figure S1 are general and to see how they depend on V_{circ}, we plot in Figure S2 the results of rotation curve decompositions illustrated in the literature[32,45–72]. The sample is from a study of dark matter scaling laws[41] augmented by more recent papers. Selection criteria are as rigorous as practical; only galaxies with H I rotation curves are used, and they need to reach large enough radii to yield reasonably reliable measures of V_{circ}. (We can never be completely certain of halo rotation velocities: it is always possible that they increase again at large radii beyond the reach of present measurements even when V_{circ} appears to have flattened out[35].) Only maximum-disk or nearly-maximum-disk decompositions and only those that are based on isothermal halos or equivalent[41] are used.

Before we interpret Figure S2, there are selection effects in the galaxy sample that we should understand. The most important one is this: H I gas needs to have been detected to large enough radii to see the rotation curve flatten. Many rotation curve decompositions were not used because they do not reach large enough radii. This requirement means that gas must be plentiful. So late Hubble types are favored. One result is that the sample of galaxies with bulges – especially small ones – is not large. However, we were able to find rotation curve decompositions for all of the galaxies shown by filled black circles in Figure 1; their points are circled in Figure S2. Also, there are notably many dwarf galaxies; this is a result of the emphasis put on studying tiny galaxies that are dominated by DM. It helps our analysis; it gives us the largest possible dynamic range for a derivation of the underlying relationship between $V_{circ,disk}$ and V_{circ} (black straight line). Finally, we note again that we use maximum disk decompositions; if disk M/L values were smaller than these maximum values, then $V_{circ,disk}$ would be correspondingly smaller. E. g., statistical comparisons of vertical velocity dispersions in face-on disks with vertical scale heights in edge-on disks suggest that M/L may be $\sim 63\,\%$ of the maximum-disk value[42,43]. Then $V_{circ,disk}$ would get $\sim 20\,\%$ smaller, $V_{circ,bulge}$ would get very slightly larger, and V_{circ} for the halo would necessarily remain unchanged. Our conclusions would be unchanged, too.

In agreement with previous work[31], we conclude that the rotation curve conspiracy works best in the biggest disk galaxies. Most galaxies with $V_{circ} \gtrsim 200$ km s^{-1} contain a large bulge, and many of these bulges are classical. Independent of whether they are classical or pseudo, $V_{circ,bulge} \simeq V_{circ,disk} \simeq V_{circ}$. At $V_{circ} \ll 200$ km s^{-1}, bulges become unimportant as V_{circ} decreases, partly because they are rarer (caution: the points in Figure S2 are not necessarily representative) and partly because $V_{circ,bulge}$ drops below the value for the halo. But these smaller galaxies are the ones for which both Figure 1 and previous work[22] show no tight $V_{circ} - \sigma$ correlation that argues for BH – DM coevolution.

We conclude that there is no compelling evidence for a direct causal correlation between BHs and DM beyond what is implied indirectly by the rotation curve conspiracy.

2. Reconstructing the $V_{circ} - \sigma$ Correlation

Figure S3 reconstructs Figure 1 for all galaxy samples discussed in this paper. The large scatter in the $V_{circ} - \sigma$ correlation reported by Ho[22] is shown by the gray points. Superposed in black are results for all rotation curve decomposition galaxies plotted in Figure S2 for which σ measurements are available. They include (circled points) all Ferrarese[6] galaxies in Figure 1 (black filled circles there) that have H I rotation curves. With the best rotation and dispersion measurements available now, their scatter is larger than it was in Figure 1 and consistent with the Ho points. Classical bulges (red) and pseudobulges (blue) that host detected BHs are included from Figure 2. They also are consistent with the Ho points. Ho also includes 18 of the 23 Ferrarese galaxies that had optical but no H I rotation data (black points marked only with error bars in Figure 1). Finally, Figure S3 shows in green the galaxies from Figure 1 that have virtually no bulge or pseudobulge; the dispersions are those of their stellar nuclei. For these, there can be no confusion with any BH – (pseudo)bulge correlation, so they remain the best galaxies with which to look for a BH – DM correlation. None is seen. Figure S3 therefore supports our conclusion that the rotation curve conspiracy is sufficient and that a conceptual leap from a BH – bulge correlation to a BH – DM correlation is not compelled by the data.

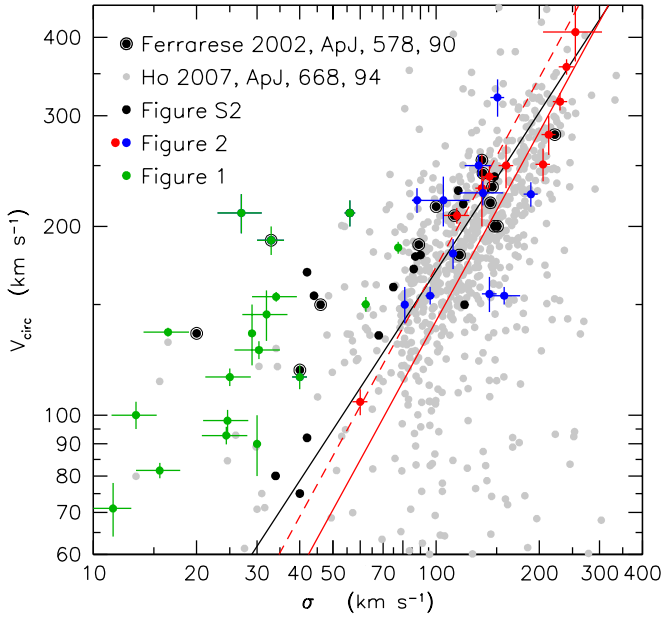

Figure S3 | Reconstruction of Figure 1 for all galaxy samples discussed in this paper. Here V_{circ} is the outer rotation velocity of the galaxy disk, usually measured using observations of H I gas, and σ is the central or near-central average velocity dispersion. Each galaxy is plotted only once; parameters are taken preferentially from Figure 1, Figure 2, Figure S2, and Ho[22]. All Ferrarese galaxies with H I measurements in Figure 1 (black filled circles there) are included here but with the best currently available parameters. Error bars are one sigma. The black straight line is Ferrarese's fit to her correlation. Ho's fit to the light gray points is not shown but is similar. The red lines are not fits; they show $V_{circ} = \sqrt{2}\,\sigma$ (lower) and $V_{circ} = 1.72\,\sigma$, respectively. The latter relation was derived[73] by fitting dynamical models with a variety of velocity anisotropies to x-ray and optical spectroscopy measurements of elliptical galaxies. An intermediate relation, $V_{circ} = 1.52\,\sigma$ (not shown) was derived[74] from a dynamical analysis of high-dynamic-range kinematic observations of ellipticals. A slope = 1 fit to the black filled circles in Figure 1 (omitting NGC 3198) gives $V_{circ} = 1.43\,\sigma$.

3. If Dark Matter Halos Predict BH Masses Independent of their Baryon Content, Then the Halos of Galaxy Clusters Predict Giant Black Holes That Are Not Seen

The main text mentions this argument briefly. We derive it here.

The original $V_{circ} - \sigma$ correlation[6], reproduced to within errors in our Figure 1 (key at the bottom), is

$$\log V_{circ} = (0.84 \pm 0.09)\,\log\sigma + (0.55 \pm 0.19)\ , \qquad (1)$$

Substituting for σ in the $M_\bullet - \sigma$ relation[6],

$$M_\bullet = (1.66 \pm 0.32) \times 10^8\ M_\odot \left(\frac{\sigma}{200\ \mathrm{km\ s^{-1}}}\right)^{4.58\pm0.52}\ , \qquad (2)$$

yields

$$\frac{M_\bullet}{10^8\ M_\odot} = 0.169 \left(\frac{V_{circ}}{200\ \mathrm{km\ s^{-1}}}\right)^{5.45} \qquad (3)$$

in our notation. As a check on previous arguments, $V_{circ} = 210$ km s^{-1} for M 101 predicts $M_\bullet \simeq 2.2 \times 10^7\ M_\odot$, in conflict with the observed upper limit[8], $M_\bullet \lesssim (2.6 \pm 0.5) \times 10^6$ M$_\odot$.

Rich clusters of galaxies have higher DM V_{circ} values than any galaxy. They typically have velocity dispersions $\sigma \sim 1000$ km s^{-1} and can have velocity dispersions as high as $\sim$ 2000 km s^{-1}. Whether we can use these cluster halos in our argument depends on whether the dark matter is already distributed in the cluster or whether it is attached only to the galaxies, with the result that the total mass is large but that individual halos are not. Large-scale simulations of hierarchical clustering show[28] that, while substructure certainly exists, much of the DM in rich, relaxed clusters is distributed "at large" in the cluster. In fact, the hierarchical clustering of DM is so nearly scale-free that[75] "*it is virtually impossible to distinguish [the halo of an individual big galaxy from that of a cluster of galaxies] even though the cluster halo is nearly a thousand times more massive*" (emphasis added). DM halos of mass 10^{15} M$_\odot$ are not rare[76]. A cluster of galaxies like Coma[77] has $\sigma \sim 1000$ km s^{-1} and $V_{circ} \sim \sqrt{2}\,\sigma \sim 1400$ km s^{-1}. Equation (3) then predicts that

$$M_\bullet \sim 7 \times 10^{11}\ M_\odot\ . \qquad (4)$$

Sunk to the center of NGC 4874 or NGC 4889, such a BH would have a sphere-of-influence radius $r_\bullet \sim GM_\bullet/\sigma^2 \simeq 34$ kpc $= 69''$. This is bigger than the effective radius of both galaxies[78]. But both galaxies have $\sigma \simeq 300$ km s^{-1} and normal, linear, and shallow $\log\sigma(\log r)$ profiles[78].

Therefore, if baryons do not matter – if the hypothesis is that DM makes BHs independent of how baryons are involved (as a galaxy, as a group of galaxies, or not at all) – then Equation (3) predicts unrealistically large M$_\bullet$ for rich clusters of galaxies.

Is this a fair argument? Does it miss some essential physics that DM requires in order to make BHs? After all, clusters are different from individual galaxies, even if both contain DM. But we emphasize: Any missing physics cannot involve the formation of bulges and ellipticals, because if those are necessary, then we are back to BH – bulge coevolution. The obvious candidate for a missing ingredient is cold gas. Rich clusters are dominated by X-ray gas. But the same is true of giant ellipticals[126], and they have manufactured the biggest BHs known. Both M 87 and the Coma cluster are dominated by stars and hot gas that are only minimally helpful for current BH growth and halos that contain some substructure but that are almost self-similar. Ferrarese (ref. 6) argues that more massive DM halos are more efficient at making BHs. The most massive halos are those of galaxy clusters. Therefore the observation that they do not contain BHs in accord with Equation (3) is a powerful argument that, absent a bulge, DM does not directly control BH growth.

TABLE 1
ROTATION VELOCITIES AND VELOCITY DISPERSIONS OF GALAXIES IN FIGURE 1

Galaxy	Type	Bulge Type	Bulge Type source	$V_{\rm circ}$ (km s^{-1})	$V_{\rm circ}$ source	σ (km s^{-1})	$\sigma_{\rm instr}$ (km s^{-1})	σ, $\sigma_{\rm instr}$ source	Figure 1 symbol
(1)	(2)	(3)	(4)	(5)	(6)	(7)	(8)	(9)	(10)
Ferrarese (2002) Galaxies With H I Rotation Curves									
MW	SBb	P	8,82,83	180 ± 20	6	100 ± 20	individual stars	98	•
IC 342	SAB(rs)cd	P,N	8,84,87	185 ± 10	6	77 ± 12	61	15	replaced
NGC 224	SA(s)b	C,N	8,85	240 ± 20	6	146 ± 15	115	99?	•
NGC 598	SA(s)cd	N	21	135 ± 13	6	27 ± 7	?	100	replaced
NGC 801	Sc	P	this paper	216 ± 9	6	144 ± 27	77	101	•
NGC 2841	SA(r)b	C	21,84,86,87	281 ± 10	6	179 ± 12	57	102	•
NGC 2903	SB(s)d	P	84,86,87	180 ± 4	6	106 ± 13	≥ 44	103	•
NGC 2998	SAB(rs)c	P	this paper	198 ± 5	6	113 ± 30	77	101	•
NGC 3198	SB(rs)c	P	86	150 ± 3	6	69 ± 13	51	93,104	replaced
NGC 3198	SB(rs)c	P	86	150 ± 3	6	48 ± 9	51,42	104,105	•
NGC 4258	SAB(s)bc	C	8,10,27	210 ± 20	6	138 ± 18	68	15	•
NGC 4565	SB(r)b	P	21,33	264 ± 8	6	151 ± 13	100	106	•
NGC 5033	SA(s)c	P	87	195 ± 5	6	122 ± 9	≥ 89	103	•
NGC 5055	SA(rs)bc	P	8,84,86,87	180 ± 5	6	103 ± 6	≥ 44	103	•
NGC 6503	SA(s)cd	P,N	8,87	116 ± 2	6	48 ± 10	34	107	replaced
NGC 7331	SA(s)b	C	21,87	239 ± 5	6	139 ± 14	78	109	•
Ferrarese (2002) Galaxies With Optical Rotation Curves									
IC 724	Sa	...	...	302 ± 3	6	243 ± 18	77	101	+
NGC 753	SAB(rs)bc	...	...	210 ± 7	6	121 ± 17	77	101	+
NGC 1353	SA(rs)bc	P	86	191 ± 6	6	92 ± 12	77	101	+
NGC 1357	SA(s)ab	...	...	259 ± 5	6	121 ± 14	77	101	+
NGC 1417	SA(r)b	...	...	240 ± 9	6	148 ± 18	77	101	+
NGC 1620	SAB(rs)bc	...	...	250 ± 4	6	123 ± 20	77	101	+
NGC 2639	(R)SA(r)A:	...	...	318 ± 4	6	195 ± 13	77	101	+
NGC 2742	SA(s)c	...	...	173 ± 4	6	63 ± 28	≥ 89	103	omitted
NGC 2775	SA(r)ab	C	84,86,87,88	270 ± 4	6	162 ± 13	77	101	+
NGC 2815	(R)SB(r)b	...	...	278 ± 3	6	199 ± 20	45	108	+
NGC 2844	SA(r)a:	...	...	171 ± 10	6	113 ± 12	77	101	+
NGC 3067	SAB(s)ab	...	...	148 ± 1	6	84 ± 29	78	109	+
NGC 3145	SB(rs)bc	...	...	261 ± 3	6	166 ± 12	77	101	+
NGC 3223	SA(r)bc	P	88	261 ± 11	6	163 ± 17	77	101	+
NGC 3593	SA(s)0/a	P	84,86,87	101 ± 4	6	56 ± 15	77	101	omitted
NGC 4062	SA(s)c	P	86,88	154 ± 13	6	90 ± 7	84	110	omitted
NGC 4321	SAB(s)bc	P	21,84,87,89	216 ± 6	6	83 ± 12	77	101	omitted
NGC 4378	(R)SA(s)a	...	...	308 ± 1	6	198 ± 18	49	101	+
NGC 4448	SB(r)ab	P	84,86,87	187 ± 3	6	175 ± 21	75	111	+
NGC 4698	SA(s)ab	?	86,87,88	252 ± 5	6	131 ± 19	78	109	+
NGC 7217	(R)SA(r)ab	C	87,88	241 ± 4	6	171 ± 17	75	111	+
NGC 7541	SB(rs)bc	...	...	179 ± 1	6	109 ± 15	?	?	omitted
NGC 7606	SA(s)b	...	...	240 ± 4	6	124 ± 21	78	109	+
Essentially (Pseudo)Bulgeless Galaxies With Nuclei									
IC 342	SAB(rs)cd	P,N	8,84,87	192 ± 3	92	33 ± 3	5.5	18	orange
NGC 598	SA(s)cd	N	16,21	135 ± 13	6	19.8 ± 0.8	8	8	red
NGC 3338	SA(s)c	P,N	8,86	186 ± 4	93	77.5 ± 1.5	8	8	red
NGC 3810	SA(rs)c	P,N	8	152 ± 3	93	62.3 ± 1.7	8	8	red
NGC 5457	SA(rs)cd	P,N	8,84	210 ± 15	8	27 ± 4	8	8	red
NGC 6503	SA(s)cd	P,N	8,87	115 ± 2	95	40 ± 2	8	8	red
NGC 6946	SA(rs)cd	P,N	8,84	210 ± 10	8	56 ± 2	8	8	red
NGC 300	SA(s)d	N	87,90	96 ± 2	96	13.3 ± 2.0	3.4	90	green
NGC 428	SAB(s)m	N	90	104 ± 11	97	24.4 ± 3.7	3.4	90	green
NGC 1042	SAB(rs)cd	N	90	145 ± 13	93	32.0 ± 4.8	3.4	90	green
NGC 1493	SB(r)cd	N	90	115 ± 4	93	25.0 ± 3.8	3.4	90	green
NGC 2139	SAB(rs)cd	N	90	136 ± 2	93	16.5 ± 2.5	3.4	90	green
NGC 3423	SA(s)cd	N	90	127 ± 4	93	30.4 ± 4.6	3.4	90	green
NGC 7418	SAB(rs)cd	N	90	154 ± 3	93	34.1 ± 5.1	3.4	90	green
NGC 7424	SAB(rs)cd	N	90	82 ± 2	93	15.6 ± 2.3	3.4	90	green
NGC 7793	SAd	N	90	96 ± 3	93	24.6 ± 3.7	3.4	90	green
NGC 1705	BCD,N	N	91	78 ± 4	93	11.4 ± 1.5	3.4	91	blue

NOTE. — The galaxies in the first two blocks are from Table 1 in reference 6; parameters are taken from there unless otherwise noted. Parameters for the third block of galaxies are from the sources listed in these notes or in the columns indicated. Column (1): Galaxy name. Column (2): Galaxy type, from reference 79 as listed in reference 80 except for NGC 1705[81]. Column (3): Bulge classification: C = classical bulge; P = pseudobulge; N = nucleus, which can occur together with C or P. Column (4): Sources of bulge classifications Column (5): Outer rotation velocity $V_{\rm circ}$. Column (6): Sources of $V_{\rm circ}$. Column (7): Adopted velocity dispersion σ. For the first two blocks of galaxies, these are reference (6) "bulge velocity dispersions corrected to an aperture of size $r_e/8$", where r_e is the radius that contains half of the light of the bulge component. Note that σ is measured in the same way whether the bulge is classical or pseudo. Column (8): Instrumental resolution of the spectrograph used to determine σ expressed as an instrumental velocity dispersion $\sigma_{\rm instr} \equiv$ FWHM/2.35, where FWHM is the full width at half of maximum intensity (or depth) of $\sigma = 0$ emission (or absorption) lines as broadened by the instrumental resolution. When $\sigma \lesssim \sigma_{\rm instr}$, the galaxy lines are dangerously under-resolved; the usual result is that σ is overestimated. A question mark in Column (6) means that the source did not give the instrumental resolution. A lower limit means that the source did not give the instrumental resolution but did give the pixel size; then (2 pixels)/2.35 is a lower limit on $\sigma_{\rm instr}$. For reference (111), we quote the "resolution width" W which is treated like an instrumental velocity dispersion in their Equation (1). Column (9): Source of σ measurements. More than half of the sources listed in reference (6) appear to be incorrect – we could not find the galaxy listed in that paper. We corrected the sources as well as possible, based on finding the paper that lists σ as given in Table 1, column (7) of reference (6). A question mark indicates that σ in the source neverthless differed from σ in reference (6). For NGC 2841, a σ value essentially equal to that in Reference (6) was found[102]. Column (10) identifies whether this measurement was used in Figure 1. Cases where σ was under-resolved are omitted when no better data are available. If better data are available, then Column (8) indicates that this line of the table was replaced with the new value in the next line (NGC 3198) or in the third block of galaxies.

4. Data Table for Galaxies in Figure 1

Table 1 lists the plotted parameters and data sources for all galaxies included in Figure 1. The top two blocks of galaxies are taken directly from reference (6) with as few changes as possible. If these points are included in Figure 1, they are plotted in black. The bottom block of galaxies (color points in Figure 1) includes only objects with no classical bulge, with very small pseudobulges (e. g., IC 342, NGC 5457, NGC 6946) or none at all (e. g., NGC 598 = M 33), and with nuclear star clusters whose velocity dispersions have been measured with very high velocity resolution ($V_{circ} < 10$ km s^{-1}). In practice, the biggest pseudobulge-to-total luminsity ratios[8] included in the bottom group of galaxies in Table 1 are PB/T ~ 0.03.

Except for two new bulge-pseudobulge classifications discussed below, all data in Table 1 are published. Column 6 lists the source of V_{circ}; this is taken directly from reference (6) – where the original source is listed – for all galaxies from that paper. The velocity dispersion σ listed by reference (6) is intended to be an average inside $r_e/8$, where r_e is the radius that contains half of the light of the bulge. Some of these values were measured with instrumental resolution $\sigma_{instr} \simeq \sigma$ which is too low (see Figure 1 caption). This is documented in Table 1: σ_{instr} is listed in Column (8) as reported in the paper that published the measurements (Column 9). When the resolution was too poor, the object was "omitted" (Column 10) if we had no better σ value or "replaced" with a high-resolution measurement, if we had one. In the latter case, the galaxy appears again, either in the next line or in the bottom block of objects, along with the high-resolution σ measurement and, when necessary, an update on V_{circ}. Many σ sources are given incorrectly in reference (6); we list these sources in Column (9), corrected as well as we are able (see Table Note for further details). Column (10) identifies the symbol used for each galaxy in Figure 1.

Readers may worry that σ is measured in different ways for the various kinds of central components included in Figures 1 and S3. But in fact, velocity dispersions σ are defined and measured in exactly the same way for pseudobulges (see below) as for classical bulges. In general, the papers that measured r_e and σ did not distinguish between classical and pseudo bulges. Nuclei are typically only a few arcsec in diameter; their σ refers to the whole nucleus. In one case (NGC 598 = M 33), measurements with the *Hubble Space Telescope* show[17] that σ is independent of radius. Then it does not matter whether σ is averaged inside $r_e/8$ or not. For NGC 5457 and NGC 6946, which contribute more than any other galaxies to our conclusion that DM halos with $V_{circ} > 200$ km s^{-1} do not contain big BHs if they do not also contain classical bulges, the nuclear σ measurement also includes an equal or larger contribution from the center of the galaxy's tiny pseudobulge[8]. In any case, nuclei are so small that, if big DM halos manufactured big BHs, then those BHs would easily be revealed by large σ values that are not seen. And velocity dispersion gradients are shallow enough so that the exact fraction of r_e inside which σ is averaged is not critical. So the comparison of colored and black points in Figure 1 is fair.

Some arguments in the main text depend critically on the distinction[10,21] between classical and pseudo bulges in the top block of galaxies – the ones that show a tight correlation in Fig. 1. Bulge classifications are less well known for the middle block of galaxies, but these are also less important, because they do not show a tight $V_{circ} - \sigma$ correlation. Table 1 lists the bulge classification in Column (3) and the source of the classification in Column (4). For NGC 801 and NGC 2998, published (pseudo)bulge classifications are not available; we discuss these galaxies next.

NGC 2998 and NGC 801 are by far the most distant galaxies in the top group in Table 1. At D = 67 Mpc and 79 Mpc, respectively, they are ~ 4 times farther away than the next most distant galaxy. As a result, much less is known about them, and in particular, bulge classifications have not been published. However, enough data are available so that we can estimate the bulge type using the shape of the surface brightness profile.

Figure S4 | Color image of the Sc galaxy NGC 2998 constructed using the g-, r-, and i-band images from the Sloan Digital Sky Survey (courtesy http://www.wikisky.org). The galaxy is a close analog of M 101, except that it is farther away (D = 67.4 Mpc versus 7.0 Mpc for M 101) and more inclined. The total K-band absolute magnitude is M_{KT} = -24.2 (compared with -23.7 for M 101). NGC 2998 has $V_{circ} = 198 \pm 5$ km s^{-1} (cf. 210 $\pm$ 15 km s^{-1} for M 101). We find a pseudobulge-to-total luminosity ratio PB/T = 0.03 $\pm$ 0.01 (cf. 0.027 $\pm$ 0.008 in M 101). The M 101 parameters are from reference (8). Error bars are 1 sigma.

NGC 2998 is illustrated in Figure S4. It is very similar to the Scd galaxy M 101, which has no classical bulge at all, but only a nuclear star cluster and a tiny pseudobulge that contributes 0.027 ± 0.008 of the K-band light of the galaxy[8]. We measured the brightness profile of NGC 2998 to see whether the tiny, bright center is a classical or pseudo bulge. The results are shown in Figure S5.

As in other normal galaxies, the outer disk has an exponential profile[114] and the central component is well fitted by a Sérsic function[113], log I(r) $\propto r^{1/n}$, where n is the "Sérsic index." The best fit has $n = 1.77 \pm 0.15$ (one sigma). This is marginally less than 2. Much work has shown[21,84,86–89,115–123] that classical bulges have $n \gtrsim 2$ whereas most pseudobulges have $n < 2$. So our results are most consistent with a pseudobulge, although a classical bulge is not strongly excluded.

NGC 801 is also classified as an Sc galaxy, but its (pseudo)bulge is brighter than that of NGC 2998. The galaxy is illustrated in Figure S6. No HST image is available, but ground-based photometry is collected into a composite profile in Figure S7.

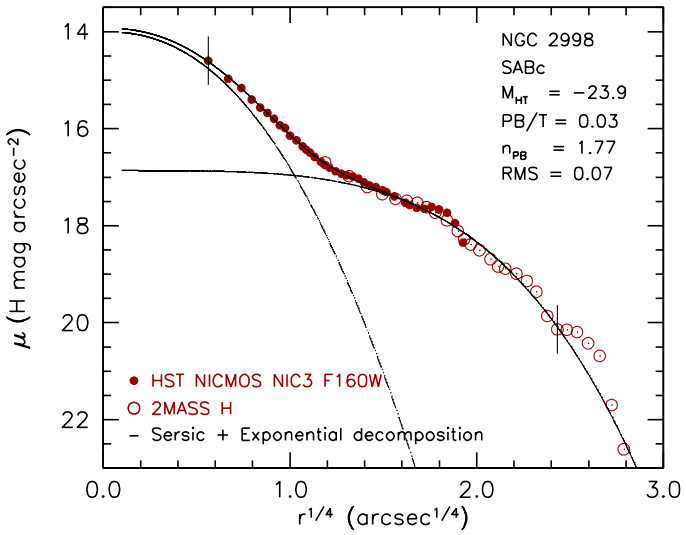

Figure S5 | Major-axis, H-band surface brightness profile of NGC 2998. The filled circles are our measurements of a Hubble Space Telescope NICMOS image available from the HST Legacy Archive, http://hla.stsci.edu/hlaview.html. The open circles are our measurments of the 2MASS H-band image[112]. The dashed curves show a decomposition of the profile into a Sérsic function[113] (pseudo)bulge and an exponential disk. Their intensity sum (solid curve) fits the average profile inside the fit range (vertical dashes) with an RMS of 0.07 mag arcsec^{-2}. The Sérsic index of the central component is n = 1.77 < 2, so we conclude that this is a pseudobulge (see the text). The pseudobulge-to-total luminosity ratio is tiny, PB/T = 0.03 ± 0.01 (one sigma).

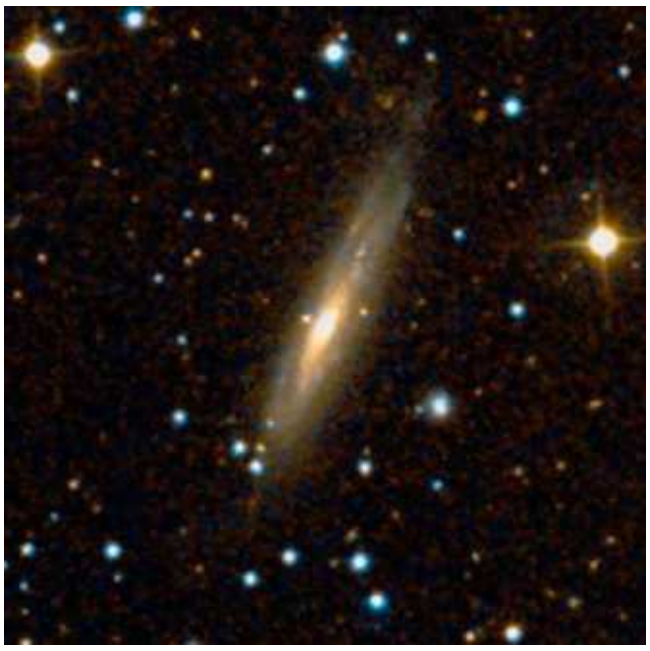

Figure S6 | Color image of the Sc galaxy NGC 801 from the Palomar Observatory and Anglo-Australian Observatory Digital Sky Survey (courtesy http://www.wikisky.org). The spatial resolution is poorer than in Figure S4; the galaxy is farther away (D = 79 Mpc), and it is almost edge-on. However, the image correctly suggests that the (pseudo)bulge contributes a larger fraction of the galaxy light than it does in NGC 2998. Otherwise, NGC 801 is also similar to M 101: M_{KT} = -25.0 and V_{circ} = 216 ± 9 km s^{-1} (one sigma).

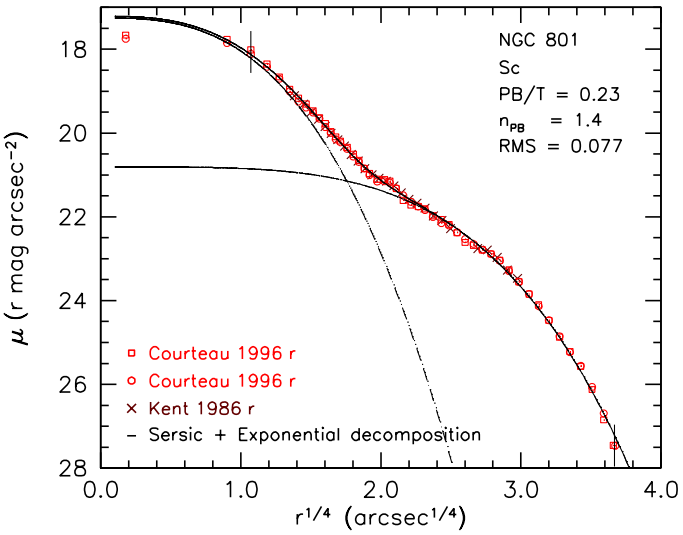

Figure S7 | Major-axis, r-band surface brightness profile[124,125] of NGC 801. The dashed curves show a decomposition into a Sérsic function and an exponential;. Their sum (solid curve) fits the profile inside the fit range (vertical dashes) with an RMS of 0.077 mag arcsec^{-2}. The Sérsic index of the central component is n = 1.4 ± 0.4 (1 sigma). It contributes ∼23 % of the galaxy light.

Our photometric decomposition (Figure S7) gives a Sérsic index that is marginally less than 2. This is most consistent with a pseudobulge, but a classical bulge is not excluded. At the large distance of this galaxy, other information such as molecular gas or star formation measurements in the central component are not available. So we cannot apply other classification criteria. We provisionally classify the bulge as pseudo but recognize that this is uncertain.

The pseudobulge classifications of NGC 801 and NGC 2998 are more uncertain than the others in the top block of Table 1, because they are based on only one classification criterion. Also, it is essentially certain that some galaxies have both a classical and a pseudo bulge component. This is unlikely in most galaxies in the top block, based on detailed studies. But it is hard to investigate in NGC 801, because that galaxy is far away and because we do not have *Hubble Space Telescope* images. (A multicomponent bulge is not likely in NGC 2998: PB/T $\simeq$ 0.03.)

However, we emphasize two points. First, if both of the above classifications were wrong, then the tight correlation of black filled circles in Figure 1 would consist of an equal number of classical bulges and pseudobulges. Our arguments in the main text would remain valid. Second, the criterion that we used to classify NGC 801 and NGC 2998 was used successfully to classify the pseudobulges that prove to show no σ – $M_\bullet$ correlation[10]. If the same classification criterion identifies a similar sample of pseudobulges that show a tight σ – DM correlation in Figure 1, than that correlation is not due to BH coevolution driven directly by DM. We discuss NGC 801 and NGC 2998 here mainly for completeness. Our conclusions do not depend on the resulting (pseudo)bulge classifications.

References

31. Casertano, S. & van Gorkom, J. H. Declining rotation curves: The end of a conspiracy? *Astron. J.* **101**, 1231–1241 (1991).
32. van Albada, T. S., Bahcall, J. N.; Begeman, K. & Sancisi, R. Distribution of dark matter in the spiral galaxy NGC 3198. *Astrophys. J.* **295**, 305–313 (1985).
33. Kormendy, J. & Barentine, J. C. Detection of a pseudobulge hidden inside the "box-shaped bulge" of NGC 4565. *Astrophys. J.* **715**, L176–L179 (2010).

34. Faber, S. M. & Gallagher, J. S. Masses and mass-to-light ratios of galaxies. *Annu. Rev. Astron. Astrophys.* **17**, 135–187 (1979).
35. Lake, G. & Feinswog, L. The distribution of dark matter in galaxies. I. Models of spiral galaxies. *Astron. J.* **98**, 166–179 (1989).
36. Athanassoula, E., Bosma, A. & Papaioannou, S. Halo parameters of spiral galaxies. *Astron. Astrophys.* **179**, 23–40 (1987).
37. Freeman, K. C. Dark matter in galaxies. in *Physics of Nearby Galaxies: Nature or Nurture?* (eds Thuan, T. X., Balkowski, C. & Van, J. T. T.) 201–214 (Éditions Frontières, 1992).
38. Debattista, V. P. & Sellwood, J. A. Dynamical friction and the distribution of dark matter in barred galaxies. *Astrophys. J.* **493**, L5–L8 (1998).
39. Debattista, V. P. & Sellwood, J. A. Constraints from dynamical friction on the dark matter content of barred galaxies. *Astrophys. J.* **543**, 704–721 (2000).
40. Weiner, B. J., Sellwood, J. A. & Williams, T. B. The disk and dark halo mass of the barred balaxy NGC 4123. II. Fluid-dynamical models. *Astrophys. J.* **546**, 931–951 (2000).
41. Kormendy, J. & Freeman, K. C. Scaling laws for dark matter halos in late-type and dwarf spheroidal galaxies. in *IAU Symposium 220, Dark Matter in Galaxies* (eds Ryder, S. D., Pisano, D. J., Walker, M. A. & Freeman, K. C.) 377–397 (Astronomical Society of the Pacific, 2004).
42. Bottema, R. The stellar kinematics of galactic disks. *Astron. Astrophys.* **275**, 16–36 (1993).
43. Bottema, R. The maximum rotation of a galactic disc. *Astron. Astrophys.* **328**, 517–525 (1997).
44. Courteau, S. & Rix, H.-W. Maximal disks and the Tully-Fisher relation. *Astrophys. J.* **513**, 561–571 (1999).
45. Kent, S. M. Dark matter in spiral galaxies. II. Galaxies with H I rotation curves. *Astron. J.* **93**, 816–832 (1987).
46. Carignan, C. & Freeman, K. C. DDO 154: A "dark" galaxy. *Astrophys. J.* **332**, L33–L36 (1988).
47. Kent, S. M. An improved bulge model for M 31. *Astron. J.* **97**, 1614–1621 (1989).
48. Jobin, M. & Carignan, C. The dark side of NGC 3109. *Astron. J.* **100**, 648–662 (1990).
49. Begeman, K. G., Broeils, A. H. & Sanders, R. H. Extended rotation curves of spiral galaxies: Dark halos and modified dynamics. *Mon. Not. R. Astron. Soc.* **249**, 523–537 (1991).
50. Puche, D. & Carignan, C. H I studies of the Sculptor group galaxies. VII. Implications on the distribution and nature of dark matter in groups. *Astrophys. J.* **378**, 487–495 (1991).
51. Broeils, A. H. *PhD thesis: Dark and visible matter in spiral galaxies* 1–255 (Rijksuniversiteit te Groningen, 1992)
52. Miller, B. W. & Rubin, V. C. Near-nuclear velocities in NGC 5907: Observations and mass models. *Astron. J.* **110**, 2692–2699 (1995).
53 Rhee, M.-H. *PhD thesis: A physical basis of the Tully-Fisher relation* 1–137 (Rijksuniversiteit te Groningen, 1996)
54. Sofue, Y. The most completely sampled rotation curves for galaxies. *Astrophys. J.* **458**, 120–131 (1996).
55. Verheijen, M. A. W. *PhD thesis: The Ursa Major cluster of galaxies* 1–254 (Rijksuniversiteit te Groningen, 1997)
56. Sicotte, V. & Carignan, C. NGC 5204: A strongly warped Magellanic spiral. II. H I kinematics and mass distribution. *Astron. J.* **113**, 609–617 (1997).
57. de Blok, W. J. G. & McGaugh, S. S. The dark and visible matter content of low surface brightness disc galaxies. *Mon. Not. R. Astron. Soc.* **290**, 533-552 (1997).
58. van Zee, L., Haynes, M. P., Salzer, J. J. & Broeils, A. H. A comparative study of star formation thresholds in gas-rich low surface brightness dwarf galaxies. *Astron. J.* **113**, 1618–1637 (1997).
59. Verdes-Montenegro, L., Bosma, A. & Athanassoula, E. The ringed, warped and isolated galaxy NGC 6015. *Astron. Astrophys.* **321**, 754–764 (1997).
60. Meurer, G. R., Staveley-Smith, L. & Killeen, N. E. B. H I and dark matter in the windy starburst dwarf galaxy NGC 1705. *Mon. Not. R. Astron. Soc.* **300**, 705–717 (1998).
61. Blais-Ouellette, S., Carignan, C., Amram, P. & Côté, S. Accurate parameters of the mass distribution in spiral galaxies. I. Fabry-Perot observations of NGC 5585. *Astron. J.* **118**, 2123–2131 (1999).
62. Côté, S., Carignan, C. & Freeman, K. C. The various kinematics of dwarf irregular galaxies in nearby groups and their dark matter distributions. *Astron. J.* **120**, 3027–3059 (2000).
63. de Blok, W. J. G. & Bosma, A. High-resolution rotation curves of low surface brightness galaxies. *Astron. Astrophys.* **385**, 816–846 (2002).
64. Corbelli, E. Dark matter and visible baryons in M 33. *Mon. Not. R. Astron. Soc.* **342**, 199–207 (2003).
65. Gentile, G., Salucci, P., Klein, U. & Granato, G. L. NGC 3741: the dark halo profile from the most extended rotation curve. *Mon. Not. R. Astron. Soc.* **375**, 199–212 (2007).
66. Noordermeer, E., van der Hulst, J. M., Sancisi, R., Swaters, R. S. & van Albada, T. S. The mass distribution in early-type disc galaxies: Declining rotation curves and correlations with optical properties. *Mon. Not. R. Astron. Soc.* **376**, 1513–1546 (2007).
67. Noordermeer, E. The rotation curves of flattened Sérsic bulges. *Mon. Not. R. Astron. Soc.* **385**, 1359–1364 (2008).
68. Dicaire, I., *et al.* Deep Fabry-Perot Hα observations of NGC 7793: A very extended Hα disk and a truly declining rotation curve. *Astron. J.* **135**, 2038–2047 (2008).
69. Yoshino, A. & Ichikawa, T. Colors and mass-to-light ratios of bulges and disks in nearby spiral galaxies. *Publ. Astron. Soc. Japan* **60**, 493–520 (2008).
70. Sofue, Y., Honma, M. & Omodaka, T. Unified rotation curve of the Galaxy – Decomposition into de Vaucourleurs bulge, disk, dark halo, and the 9-kpc rotation dip. *Publ. Astron. Soc. Japan* **61**, 227–236 (2009).
71. Puglielli, D., Widrow, L. M. & Courteau, S. Dynamical models for NGC 6503 using a Markov chain Monte Carlo technique. *Astrophys. J.* **715**, 1152–1169 (2010).
72. Elson, E. C., de Blok, W. J. G. & Kraan-Korteweg, R. C. The dark matter content of the blue compact dwarf NGC 2915. *Mon. Not. R. Astron. Soc.* **404**, 2061–2076 (2010).
73. Churazov, E., *et al.* Comparison of approximately isothermal gravitational potentials of elliptical galaxies based on x-ray and optical data. *Mon. Not. R. Astron. Soc.* **404**, 1165–1185 (2010).
74. Gerhard, O., Kronawitter, A., Saglia, R. P. & Bender, R. Dynamical family properties and dark halo scaling relations of giant elliptical galaxies. *Astron. J.* **121**, 1936–1951 (2001).
75. Moore, B., Ghigna, S., Governato, F., Lake, G., Quinn, T. & Stadel, J. Dark matter substructure within galactic halos. *Astrophys. J.* **524**, L19–L22 (1999).
76. Faltenbacher, A., Finoguenov, A. & Drory, N. The halo mass function conditioned on density from the Millennium Simulation: Insights into missing baryons and galaxy mass functions. *Astrophys. J.* **712**, 484–493 (2010).
77. Kent, S. M. & Gunn, J. E. The dynamics of rich clusters of galaxies. I. The Coma Cluster. *Astron. J.* **87**, 945–971 (1982).
78. Fisher, D., Illingworth, G. & Franx, M. Kinematics of 13 brightest cluster galaxies. *Astrophys. J.* **438**, 539–562 (1995).
79. de Vaucouleurs, G., de Vaucouleurs, A., Corwin, H. G., Buta, R. J., Paturel, G. & Fouqué, P. *Third Reference Catalogue of Bright Galaxies*. (Springer, 1991).
80. NASA/IPAC Extragalactic Database (NED), http://nedwww.ipac.caltech.edu/
81. Meurer, G. R., Freeman, K. C., Dopita, M. A. & Cacciari, C. NGC 1705. I. Stellar populations and mass loss via a galactic wind. *Astron. J.* **103**, 60–80 (1992).
82. Howard, C. D., *et al.* Kinematics at the edge of the Galactic bulge: Evidence for cylindrical rotation. *Astrophys. J.* **702**, L153–L157 (2009).
83. Shen, J., Rich, R. M., Kormendy, J., Howard, C. D., De Propris, R. & Kunder, A. Our Milky Way as a pure-disk galaxy – A challenge for galaxy formation. *Astrophys. J.* **720**, L72–L76 (2010).
84. Fisher, D. B., Drory, N. & Fabricius, M. H. Bulges of nearby galaxies with Spitzer: The growth of pseudobulges in disk galaxies and its connection to outer disks. *Astrophys. J.* **697**, 630–650 (2009).
85. Kormendy, J. & Bender, R. The double nucleus and central black hole of M31. *Astrophys. J.* **522**, 772–792 (1999).
86. Fisher, D. B. & Drory, N. The structure of classical bulges and pseudobulges: The link between pseudobulges and Sérsic index. *Astron. J.* **136**, 773–839 (2008).
87. Fisher, D. B. & Drory, N. Bulges of nearby galaxies with Spitzer: Scaling relations in pseudobulges and classical bulges. *Astrophys. J.* **716**, 942–969 (2010).
88. Weinzirl, T., Jogee, S., Khochfar, S., Burkert, A. & Kormendy, J. Bulge n and B/T in high-mass galaxies: Constraints on the origin of bulges in hierarchical models. *Astrophys. J.* **696**, 411–447 (2009).
89. Kormendy, J. & Cornell, M. E. Secular evolution and the growth of pseudobulges in disk galaxies. in *Penetrating bars through masks of cosmic dust: The Hubble tuning fork strikes new note.* (eds Block, D. L., Puerari, I., Freeman, K. C., Groess, R. & Block, E. K.) 261–280 (Kluwer, 2004).
90. Walcher, C. J., van der Marel, R. P., McLaughlin, D., Rix, H.-W., Böker, T., Häring, N., Ho, L. C., Sarzi, M. & Shields, J. C. Masses of star clusters in the nuclei of bulgeless spiral galaxies. *Astrophys. J.* **618**, 237–246 (2005).
91. Ho, L. C. & Filippenko, A. V. High-dispersion spectroscopy of a luminous, young star cluster in NGC 1705: Further evidence for present-day formation of globular clusters. *Astrophys. J.* **472**, 600–610 (1996).

92. Sofue, Y. The most completely sampled rotation curves for galaxies. *Astrophys. J.* **458**, 120–131 (1996).
93. HyperLeda database: http://leda.univ-lyon1.fr, see reference 94.
94. Paturel, G., Petit, C., Prugniel, Ph., Theureau, G., Rousseau, J., Brouty, M., Dubois, P. & Cambrésy, L. HYPERLEDA. I. Identification and designation of galaxies. *Astron. Astrophys.* **412**, 45–55 (2003).
95. van Moorsel, G. A. & Wells, D. C. Analysis of high-resolution velocity fields – NGC 6503. *Astron. J.* **90**, 1038–1045 (1985).
96. Puche, D., Carignan, C. & Bosma, A. H I studies of the Sculptor Group galaxies. VI. NGC 300. *Astron. J.* **100**, 1468–1476 (1990).
97. Epinat, B., Amram, P. & Marcelin, M. 2008. GHASP: An Hα kinematic survey of 203 spiral and irregular galaxies. VII. Revisiting the analysis of Hα data cubes for 97 galaxies. *Mon. Not. R. Astron. Soc.* **390**, 466–504 (2008).
98. Merritt, D. & Ferrarese, L. The $M_\bullet$–σ relation for supermassive black holes. *Astrophys. J.* **547**, 140–145 (2001).
99. Whitmore, B. C. & Kirshner, R. P. Velocity dispersions in the bulges of spiral and S0 galaxies. II. Further observations and a simple three-component model for spiral galaxies. *Astrophys. J.* **250**, 43–54 (1981).
100. Merritt, D., Ferrarese, L. & Joseph, C. L. No supermassive black hole in M33? *Science* **293**, 1116–1118 (2001).
101. Schechter, P. L. New central velocity dispersions for the bulges of 53 spiral and S0 galaxies. *Astrophys. J. Suppl. Ser.* **52**, 425–427 (1983).
102. Vega Beltrán, J. C., Pizzella, A., Corsini, E. M., Funes, J. G., Zeilinger, W. W., Beckman, J. E. & Bertola, F. Kinematic properties of gas and stars in 20 disc galaxies. *Astron. Astrophys.* **374**, 394–411 (2001).
103. Héraudeau, Ph. & Simien, F. Stellar kinematical data for the central region of spiral galaxies. I. *Astron. Astrophys. Suppl. Ser.* **133**, 317–323 (1998).
104. Bottema, R. The stellar kinematics of the spiral galaxies NGC 3198 and NGC 3938. *Astron. Astrophys.* **197**, 105–122 (1988).
105. Ho, L. C., Greene, J. E., Filippenko, A. V. & Sargent, W. L. W. A search for "dwarf" Seyfert nuclei. VII. A catalog of central stellar velocity dispersions of nearby galaxies. *Astrophys. J. Suppl. Ser.* **183**, 1–16 (2009).
106. Kormendy, J. & Illingworth, G. Rotation of the bulge components of disk galaxies. *Astrophys. J.* **256**, 460–480 (1982).
107. Bottema, R. The stellar velocity dispersion of the spiral galaxies NGC 6503 and NGC 6340. *Astron. Astrophys.* **221**, 236–249 (1989).
108. Bottema, R. The stellar velocity dispersion of the spiral galaxies NGC 1566 and NGC 2815. *Astron. Astrophys.* **257**, 69–84 (1992).
109. Héraudeau, Ph., Simien, F., Maubon, G. & Prugniel, Ph. Stellar kinematic data for the central region of spiral galaxies. II. *Astron. Astrophys. Suppl. Ser.* **136**, 509–514 (1999).
110. Whitmore, B. C., Rubin, V. C. & Ford, W. K. Stellar and gas kinematics in disk galaxies. *Astrophys. J.* **287**, 66–79 (1984).
111. Whitmore, B. C., Kirshner, R. P. & Schechter, P. L. Velocity dispersions in the bulges of spiral galaxies. *Astrophys. J.* **234**, 68–75 (1979).
112. Jarrett, T. H., Chester, T., Cutri, R., Schneider, S. E. & Huchra, J. P. The 2MASS Large Galaxy Atlas. *Astron. J.* **125**, 525–554 (2003).
113. Sérsic, J. L. *Atlas de Galaxias Australes*. (Observatorio Astronómico, Universidad Nacional de Córdoba, 1968)
114. Freeman, K. C. 1970, On the disks of spiral and S0 galaxies. *Astrophys. J.* **160**, 811–830 (1970).
115. Courteau, S., de Jong, R. S. & Broeils, A. H. Evidence for secular evolution in late-type spirals. *Astrophys. J.* **457**, L73–L76 (1996).
116. Carollo, C. M., Stiavelli, M. & Mack, J. Spiral galaxies with WFPC2. II. The nuclear properties of 40 objects. *Astron. J.* **116**, 68–84 (1998).
117. Carollo, C. M., Stiavelli, M., de Zeeuw, P. T., Seigar, M. & Dejonghe, H. Hubble Space Telescope optical–near-infrared colors of nearby $r^{1/4}$ and exponential bulges. *Astrophys. J.* **546**, 216–222 (2001).
118. MacArthur, L. A., Courteau, S. & Holtzman, J. A. Structure of disk-dominated galaxies. I. Bulge/disk parameters, simulations, and secular evolution. *Astrophys. J.* **582**, 689–722 (2003).
119. Balcells, M., Graham, A. W., Domínguez-Palmero, L. & Peletier, R. F. Galactic bulges from Hubble Space Telescope near-infrared camera multi-object spectrometer observations: The lack of $r^{1/4}$ bulges. *Astrophys. J.* **582**, L79–L82 (2003).
120. Fathi, K. & Peletier, R. F. Do bulges of early- and late-type spirals have different morphology? *Astron. Astrophys.* **407**, 61–74 (2003).
121. Scarlata, C., *et al.* Nuclear properties of a sample of nearby spiral galaxies from Hubble Space Telescope STIS imaging. *Astron. J.* **128**, 1124–1137 (2004).
122. Gadotti, D. A. Structural properties of pseudo-bulges, classical bulges and elliptical galaxies: A Sloan Digital Sky Survey perspective *Mon. Not. R. Astron. Soc.* **393**, 1531–1552 (2009).
123. Ganda, K., Peletier, R. F., Balcells, M. & Falcón-Barroso, J. The nature of late-type spiral galaxies: Structural parameters, optical and near-infrared colour profiles and dust extinction. *Mon. Not. R. Astron. Soc.* **395**, 1669–1694 (2009).
124. Courteau, S. Deep r-band photometry for northern spiral galaxies. *Astrophys. J. Suppl. Ser.* **103**, 363–426 (1996).
125. Kent, S. M. Dark matter in spiral galaxies. I. Galaxies with optical rotation curves. *Astron. J.* **91**, 1301–1327 (1986).
126. Kormendy, J., Fisher, D. B., Cornell, M. E. & Bender, R. Structure and formation of elliptical and spheroidal galaxies. *Astrophys. J. Suppl. Ser.* **182**, 216–309 (2009).